Published in final edited form as:
Eur J Med Chem. 2012 December ; 58: 390–395. doi:10.1016/j.ejmech.2012.10.028.

Hesperetin: an Inhibitor of the Transforming Growth Factor-β (TGF-β) Signaling Pathway

Yong Yang[1,*], **Joy Wolfram**[1], **Haifa Shen**[1], **Xiaohong Fang**[2], and **Mauro Ferrari**[1,*]

[1]Department of Nanomedicine, The Methodist Hospital Research Institute, Houston, TX 77030, USA.

[2]Beijing National Laboratory for Molecular Sciences, Institute of Chemistry, Key Laboratory of Molecular Nanostructures and Nanotechnology, Chinese Academy of Sciences, Beijing 100190, PR China.

Abstract

We have identified a previously unknown function of the natural compound, hesperetin. Here, we demonstrate that this small molecular agent is able to inhibit the transforming growth factor-β (TGF-β) signaling pathway. Single-molecule force measurements and single-molecule fluorescence imaging show that hesperetin interferes with ligand-receptor interactions. Furthermore, by Western blot analysis, it was confirmed that hesperetin also inhibits the phosphorylation of Smad3, a down-stream target of the TGF-β pathway. In addition we demonstrated that this compound hinders TGF-β1-induced cancer cell migration and invasion. These results suggest a potential future application for hesperetin as a TGF-β inhibitor in cancer therapy.

Keywords

hesperetin; TGF-β inhibition

1. Introduction

Hesperetin (4′-methoxy-3′,5,7-trihydroxyflavanone), a natural predominant flavanone found in citrus fruits and used in Chinese medicine, has previously been shown to have anti-cancer activity by inhibiting proliferation/inducing apoptosis [1–5], inhibiting angiogenesis [2, 6] and by acting as an anti-oxidant [7–9]. Here we examine the effect of hesperetin on the transforming growth factor-β (TGF-β) pathway. TGF-β signaling is initiated by the binding of a ligand to TGF-β receptors, which thereby form a heteromeric signaling complex. This leads to the phosphorylation of a subset of downstream signaling molecules, the receptoractivated Smads, which regulate the transcription of target genes[10, 11].

*Corresponding author. Tel.: +7134414117; yyang@tmhs.org.

Conflicts of Interest

All authors declare no competing financial interests.

We have previously shown that naringenin, another citrus bioflavonoid, is able to block the TGF-β pathway [12]. In this study, we demonstrate that hesperetin likewise inhibits TGF-β signaling, and furthermore we show that this inhibition blocks the metastatic properties of cancer cells. To date, there are several synthetic inhibitors of the TGF-β signaling pathway that are at the pre-clinical or clinical level [13–16]. These agents are powerful tools for understanding and targeting signal transduction pathways involved in pathological processes. Hesperetin and naringenin represent a new group of agents that can suppress the TGF-β pathway, and could potentially have several advantages compared to their synthetic counterparts (i.e. lower toxicity, unique mechanism of inhibition and multiple advantageous effects).

2. Results and Discussion

2.1. TGF-β Ligand-Receptor Binding

To determine whether hesperetin affects ligand-receptor interactions we performed single-molecule force spectroscopy in living cells, measuring the binding force and binding probability of TGF-β1 and TGF-β type II receptor (TβRII). The ligand was attached to the atomic force microscopy (AFM) tip and then inserted onto HeLa cells, which naturally express TβRII (Figure 1a-b). The rupture force was measured by moving the tip in and out of contact with the cell surface. The rupture force was identified as a sudden deviation in the smooth force curve [17]. To confirm that the measured forces were specific to the ligand-receptor pair of interest, the extracellular domain of TβRII (TβRII-ECD) was added as a control (Figure S1a). Force distribution histograms were shown to display a single maximum peak with a Gaussian fit, indicating that single-molecule forces were measured (Figure S1b-c). The frequency of adhesion events was low, thereby, ensuring that the force was mediated by a single ligand-receptor pair (<30% adhesion events: >85% probability of single-molecule force measurement) [18–20]. The results indicate that the addition of hesperetin to cell culture lowers the probability that the ligand will bind to the receptor (vehicle: 23.4%±2.5%, hesperetin: 10.5%±1.7%) (Figure 1c). When binding does occur, however, the rupture force is similar to that of the control (Figure S1b-c). To further confirm that hesperetin inhibits the interaction between the ligand-receptor pair, flow cytometry was performed using biotinylated TGF-β1 and avidin-FITC. Figure 1d demonstrates that the fluorescence signal decreases in the presence of hesperetin.

2.2. TGF-β Receptor Dimerization

It is known that the TGF-β receptors exist as monomers at low expression levels, and follow the general ligand-induced receptor dimerization model for activation upon TGF-β1 stimulation [21, 22]. Here we have used total internal reflection fluorescence microscopy (TIRFM) to image individual GFP-tagged TβRII molecules on the cell membrane, in order to examine the effect of hesperetin on dimer formation. As shown in a typical TIRFM image of resting HeLa cells (Figure 2a and Movie S1), TβRII-GFP molecules appear as well-dispersed diffraction-limited fluorescent spots (5×5 pixels, 800×800 nm). The fluorescence intensities of these spots were usually maintained for less than five seconds after dropping back to background level, indicating that they are single TβRII molecules. The fluorescence intensity distribution of the spots exhibited a sum of two Gaussian distributions (Figure S2a). The first population, representing TβRII monomers, had peak intensity close to that of a single GFP molecule (Figure S2c), while the second population, corresponding to TβRII dimers, had a peak value of approximately twice this size (Figure S2a). Upon addition of hesperetin to ligand-stimulated cells the percentage of dimers decreased from 40.2% to 19.9% (Figure 2b-c). In the absence of TGF-β1, hesperetin was unable to affect receptor dynamics (Figure S2a-b). An alternative way to examine dimer formation is by utilizing the bleaching-step counting method, where one-step photobleaching spots represent monomers

and two-step spots represent dimers (Figure S3)[21–23]. With this technique we show that hesperetin lowers the frequency of dimmers (control: 39.9±2.5%, hesperetin: 19.5±1.5%) (Figure 2d).

2.3. TGF-β Downstream Signaling

In order to confirm that hesperetin inhibits TGF-β signaling transduction, protein levels of the down-stream molecule, phosphorylated Smad3, were investigated. The result demonstrates that hesperetin effectively reduces the TGF-β1 induced phosphorylation of Smad3 in HeLa cells (Figure 3a). Furthermore, in the presence of TGF-β1 hesperetin administration significantly decreases the nuclear translocation of Smad3 (Figure 3b). To further investigate the effect of hesperetin on TGF-β1 downstream signaling we also examined the expression of p21, an inhibitor of cell cycle progression. Previous reports have shown that TGF-β1 stimulation leads to an increase in the expression of p21 [24]. Our results demonstrate that hesperetin significantly inhibits TGF-β1 stimulated expression of p21 (Figure 3c).

2.4. Cell Invasion and Migration

There is a controversy surrounding the role of the TGF-β pathway in cancer progression. Although the TGF-β signaling cascade suppresses tumor growth in early carcinogenesis, mainly through the ability of TGF-β to inhibit the cell cycle, it paradoxically favors tumor progression during late-stage metastasis [25]. To better understand the inhibitory effect of hesperetin on TGF-β signaling propagation we investigated the effects of this agent on TGF-β1-induced cell invasion and scattering. A scratch motility assay demonstrates that starved untreated HeLa cells exhibit only limited wound closure activity, while TGF-β1 treated cells show an acceleration of wound closure. However, when adding hesperetin (100 μM, 24 hours), the cell migration capacity was reduced (Figure 4a-b). The ability of hesperetin to prevent TGF-β1 induced invasion was similarly examined. By using the Boyden chamber assay it was confirmed that hesperetin also suppresses the cells ability to invade across a collagen matrix. (Figure 4c). Furthermore, we show that hesperetin has low cellular toxicity when used in a similar manner as in the migration assays (Figure S4).

3. Conclusion

In summary, we have discovered a novel TGF-β signaling antagonist and verified its function by single-molecule fluorescence microscopy and force spectroscopy. Our results demonstrate that hesperetin reduces the binding probability of TGF-β1 to its receptor TβRII, thereby reducing receptor dimerization and activation. We further demonstrate that the downstream signal transduction event of Smad3 phosphorylation is inhibited. Moreover, cell scattering and invasion experiments reveal that hesperetin has the potential to become an anticancer agent for the inhibition of TGF-β induced tumor progression.

4. Experimental Protocols

4.1. Cell Culture

HeLa cells were cultured with Dulbecco Modified Eagle Medium (DMEM) (Gibco) supplemented with 10% fetal bovine serum (FBS) (HyClone). Cells were maintained at 37°C and 5% CO_2.

4.2. Atomic Force Microscopy (AFM)

Atomic force microscopy (AFM) was used to measure the binding force between transforming growth factor-β1 (TGF-β1) and TGF-β type II receptor (TβRII). The AFM tip (type: NP, from Veeco, Santa Barbara, CA, USA) with TGF-β1 was prepared as previously

reported [18, 20]. The force was measured with a PicoSPM II, a PicoScan 3000 controller, a large scanner (Molecular Imaging, Tempe, AZ) and an inverted fluorescence microscope (Olympus IX71, Japan). The loading rate of force measurements was 1.0×10^4 pN/s. The force curves were recorded and analyzed by PicoScan 5 software (Molecular Imaging, Tempe, AZ). All forces were measured in living HeLa cells with contact mode at room temperature. Cells were treated with vehicle (0.1% dimethyl sulfoxide (DMSO)) or hesperetin (100 μM) or the extracellular domain of TβRII for one hour.

4.3. Flow Cytometry

Flow cytometry was used to measure the binding of TGF-β1 to TβRII. TGF-β was labeled using the Fluorokine TGF-β-biotin kit (R&D Systems) according to manufacturer's instructions. HeLa cells were incubated with vehicle (0.1% DMSO) or hesperetin (100μM), in the presence of biotinylated TGF-β1 for one hour.

4.4. Single-Molecule Fluorescence Microscopy

Single-molecule fluorescence microscopy was performed to study TβRII dimerization. A TβRII-GFP expression plasmid was created by subcloning the gene into the HindIII and BamHI sites of pEGFP-N1 (Clontech) [12, 21, 22]. Cells were cultured in 35-mm glass-bottom dishes (MatTek Corporation) and transfected with 0.2 μg/mL plasmids in phenol red-free DMEM using lipofectamine2000 (Invitrogen). To achieve low-level protein expression cells were incubated with the plasmid for four hours. Cells received either vehicle (0.1% DMSO) or 100 μM hesperetin (Sigma Aldrich) for one hour before imaging. For ligand stimulation the transfected cells were incubated for an additional 15 minutes with 10 ng/mL TGF-β1 (R&D). The fluorescence intensity measurements were performed on living cells with a CO_2 incubation system (INU-ZIL-F1, TOKAI HIT), while the photobleaching study was done on fixed cells (4% paraformaldehyde/PBS solution, 10 minutes). The intensity of single GFP molecules was measured to confirm that it corresponded to that of TβRII monomers. GFP protein was purified from *E. coli* and dissolved in a high salt buffer (600 mM NaCl, 150 mM PBS buffer, pH 7.4) to prevent dimer formation and then immobilized on coverslips through a biotin coupled GFP antibody (Clontech), as previously reported [12, 21, 22].

Single-molecule fluorescence imaging was carried out using an inverted microscope (IX 71, Olympus, Japan) with a total internal reflective fluorescence illuminator, a 100X/1.45NA Plan Apochromat TIR objective (Olympus, Japan) and a 14-bit back-illuminated electron-multiplying charge-coupled device (EMCCD) (Andor iXon DU-897 BV) [12, 21, 22]. A 488-nm argon laser with the power of 5 mW (Melles Griot, Carlsbad, CA) was used to excite the GFP in epi-fluorescence mode. Before being directed into the EMCCD (gain: 300) the fluorescent signals were passed through two filters, BA510IF and HQ 525/50 (Chroma Technology). To insure homogeneous illumination only the central quarter of the chip (256×256 pixels) was used for imaging analysis. MetaMorph software (Molecular Device) was used to acquire and analyze movies (200 frames for each sample at a frame rate of 10 Hz). The background fluorescence was first subtracted from each frame using the rolling ball method in Image J software (National Institute of Health). The first frame of each movie was used for the selection of fluorescent spots and the threshold was set a four times that of the mean intensity of an area lacking fluorescent spots. The image was then filtered again with a user-defined program in Matlab.

4.5. Western Blotting

Western blotting was performed in order to study downstream signaling of the TGF-β pathway. For detection of Smad3, the starved HeLa cells were treated with vehicle (0.1% DMSO) or hesperetin (100μM) for 1 hour in the absence or presence of TGF-β1. For the

detection of p21, the starved HeLa cells were treated with vehicle (0.1% DMSO) or hesperetin (100μM) for 24 hours in the absence or presence of TGF-β1. Cells were resuspended in 200 μl of 0.9% saline with protease inhibitors (1 mM phenylmethylsulfonyl fluoride, 10 μg/ml aprotinin, 10 μg/ml leupeptin, and 10 μg/ml pepstatin A) and mixed with 200 μl double-strength Laemmli buffer (100 mM Tris-HCl, pH 6.8, 200 mM dithiothreitol, 4% SDS, 0.2% bromophenol blue, and 20% glycerol). Cell lysates were denatured for 10 minutes at 95°C. Cell lysates were were separated by SDS gel electrophoresis (7.5% SDS gels) and transferred to polyvinylidene fluoride (PVDF membranes) with 0.192 M glycine, 0.025 M Tris and 20% methanol. Membranes were saturated for one hour at 4°C in TBS, pH 7.4, containing 5% nonfat milk and probed for two hours at room temperature with primary antibodies for p-Smad3 (Cell Signaling, dilution 1:1000), Smad3 (Cell Signaling, dilution 1:1000) or p21 (Cell Signaling, dilution 1:1000). After washing the blots were probed for one hour at room temperature with a peroxidase-conjugated secondary antibodies. Antibody binding was detected by enhanced chemiluminescence (Amersham Life Sciences, Amersham, UK).

4.6. Immunofluorescence Imaging

HeLa cells were cultured in 35 mm dishes for a period of 24 hours, followed by washing with PBS, and incubation with fresh serum-free medium for another 24 hours. The nuclear translocation of Smad3 was assessed by treating cells with 0.1% DMSO (vehicle) or hesperetin (100 μM) for 1 hour, in the absence or presence of TGF-β1. Cells were then fixed with 4% paraformaldehyde and permeabilized with 0.1% Triton X-100. 1% BSA in PBST (PBS containing 0.1% Tween-20) was used to block nonspecific binding sites. The fixed cells were then incubated with Smad3 monoclonal rabbit primary antibody overnight (Cell Signaling, 1:200 dilution), followed by washing and a 1 hour incubation with Alexa 488-conjugated anti-rabbit IgG secondary antibody (Invitrogen, 1:500 dilution). All antibodies were diluted in PBST solution containing 1% BSA. Fluorescence imaging was performed with a confocal microscope (Olympus IX81).

4.7. Scratch Motility and Invasion Assay

Scratch motility and invasion assays were performed to investigate TGF-β1-induced cell migration. Cells were grown overnight to confluency in serum-containing DMEM and then starved for 24 hours. For the scratch motility assay 1×10^6 cells were seeded in a 6-well plate. The monolayer was scratched with a pipette tip and washed with PBS to remove floating cells. The cells then received either vehicle (0.1% DMSO) or hesperetin (100μM) with or without TGF-β1 for 24 hours. Five randomly selected fields in the scratched area were photographed and the mean amount of cells/field was calculated. For the invasion assay the cells (1×10^6 cells/ml) were suspended in serum-free media and treated with vehicle and hesperetin, as mentioned above. The assay was performed in triplicates using QCMTM 24-Well Collagen-Based Cell Invasion Assay (Millipore), according to the manufacturer's instructions.

4.8. Cell Proliferation Assay

HeLa cells were seeded in 96-well plates (1×10^4 cells/well) with complete medium for 24 hours, followed by treatment with vehicle (0.1% DMSO) or 0–200 μM of hesperetin for 24 hours. Cellular proliferation was quantified using the CellTiter 96® AQueous Non-Radioactive Cell Proliferation Assay (Promega Corporation), according to the manufacturer's instructions.

4.9. Statistical Analysis

The data is expressed as the mean and standard deviation (S.D). Statistical significance was measured with the Student's *t*-test (unpaired and two-tailed) (Microsoft Excel).

Supplementary Material

Refer to Web version on PubMed Central for supplementary material.

Acknowledgments

The authors acknowledge supports from the following funding sources: Ernest Cockrell Jr. Distinguished Endowed Chair (M.F.), US Department of Defense (W81XWH-09-1-0212) (M.F.), National Institute of Health (U54CA143837, U54CA151668) (M.F.), National Basic Research Program of China (2007CB935601) (X.F.), National Natural Science Foundation of China (Nos 90713024, 20821003) (X.F.), Chinese Academy of Sciences (X.F.) and Nylands nation Finland (J.W.).

References

1. Choi EJ. Hesperetin induced G1-phase cell cycle arrest in human breast cancer MCF-7 cells: involvement of CDK4 and p21. Nutr Cancer. 2007; 59:115–119. [PubMed: 17927510]
2. Nalini N, Aranganathan S, Kabalimurthy J. Chemopreventive efficacy of hesperetin (citrus flavonone) against 1,2-dimethylhydrazine-induced rat colon carcinogenesis. Toxicol Mech Methods. 2012
3. Patil JR, Chidambara Murthy KN, Jayaprakasha GK, Chetti MB, Patil BS. Bioactive compounds from Mexican lime (Citrus aurantifolia) juice induce apoptosis in human pancreatic cells. J Agric Food Chem. 2009; 57:10933–10942. [PubMed: 19919125]
4. Sivagami G, Vinothkumar R, Preethy CP, Riyasdeen A, Akbarsha MA, Menon VP, Nalini N. Role of hesperetin (a natural flavonoid) and its analogue on apoptosis in HT-29 human colon adenocarcinoma cell line--a comparative study. Food Chem Toxicol. 2012; 50:660–671. [PubMed: 22142698]
5. Zarebczan B, Pinchot SN, Kunnimalaiyaan M, Chen H. Hesperetin, a potential therapy for carcinoid cancer. Am J Surg. 2011; 201:329–332. discussion 333. [PubMed: 21367373]
6. Choi EJ, Kim GD, Chee KM, Kim GH. Effects of hesperetin on vessel structure formation in mouse embryonic stem (mES) cells. Nutrition. 2006; 22:947–951. [PubMed: 16815676]
7. Cho J. Antioxidant and neuroprotective effects of hesperidin and its aglycone hesperetin. Arch Pharm Res. 2006; 29:699–706. [PubMed: 16964766]
8. Haidari F, Ali Keshavarz S, Reza Rashidi M, Mohammad Shahi M. Orange juice and hesperetin supplementation to hyperuricemic rats alter oxidative stress markers and xanthine oxidoreductase activity. J Clin Biochem Nutr. 2009; 45:285–291. [PubMed: 19902018]
9. Yang HL, Chen SC, Senthil Kumar KJ, Yu KN, Lee Chao PD, Tsai SY, Hou YC, Hseu YC. Antioxidant and anti-inflammatory potential of hesperetin metabolites obtained from hesperetin-administered rat serum: an ex vivo approach. J Agric Food Chem. 2012; 60:522–532. [PubMed: 22098419]
10. Massague J, Chen YG. Controlling TGF-beta signaling. Genes Dev. 2000; 14:627–644. [PubMed: 10733523]
11. ten Dijke P, Hill CS. New insights into TGF-beta-Smad signalling. Trends Biochem Sci. 2004; 29:265–273. [PubMed: 15130563]
12. Yang Y, Xu Y, Xia T, Chen F, Zhang C, Liang W, Lai L, Fang X. A single-molecule study of the inhibition effect of Naringenin on transforming growth factor-beta ligand-receptor binding. Chem Commun (Camb). 2011; 47:5440–5442. [PubMed: 21475751]
13. Flavell RA, Sanjabi S, Wrzesinski SH, Licona-Limon P. The polarization of immune cells in the tumour environment by TGFbeta. Nat Rev Immunol. 2010; 10:554–567. [PubMed: 20616810]
14. Yingling JM, Blanchard KL, Sawyer JS. Development of TGF-beta signalling inhibitors for cancer therapy. Nat Rev Drug Discov. 2004; 3:1011–1022. [PubMed: 15573100]

15. Jin CH, Sreenu D, Krishnaiah M, Subrahmanyam VB, Rao KS, Nagendra Mohan AV, Park CY, Son JY, Son DH, Park HJ, Sheen YY, Kim DK. Synthesis and biological evaluation of 1-substituted-3(5)-(6-methylpyridin-2-yl)-4-(quinoxalin-6-yl)pyrazoles as transforming growth factor-beta type 1 receptor kinase inhibitors. Eur J Med Chem. 2011; 46:3917–3925. [PubMed: 21696866]

16. Kim DK, Jung SH, Lee HS, Dewang PM. Synthesis and biological evaluation of benzenesulfonamide-substituted 4-(6-alkylpyridin-2-yl)-5-(quinoxalin-6-yl)imidazoles as transforming growth factor-beta type 1 receptor kinase inhibitors. Eur J Med Chem. 2009; 44:568–576. [PubMed: 18467006]

17. Yang H, Yu J, Fu G, Shi X, Xiao L, Chen Y, Fang X, He C. Interaction between single molecules of Mac-1 and ICAM-1 in living cells: an atomic force microscopy study. Exp Cell Res. 2007; 313:3497–3504. [PubMed: 17803991]

18. Shi X, Xu L, Yu J, Fang X. Study of inhibition effect of herceptin on interaction between heregulin and erbB receptors HER3/HER2 by single-molecule force spectroscopy. Exp Cell Res. 2009; 315:2847–2855. [PubMed: 19497323]

19. Sun S, Yu JP, Chen F, Zhao TJ, Fang XH, Li YQ, Sui SF. TINY, a dehydration-responsive element (DRE)-binding proteinlike transcription factor connecting the DRE- and ethylene-responsive element-mediated signaling pathways in Arabidopsis. J Biol Chem. 2008; 283:6261–6271. [PubMed: 18089556]

20. Yu J, Wang Q, Shi X, Ma X, Yang H, Chen YG, Fang X. Single-molecule force spectroscopy study of interaction between transforming growth factor beta1 and its receptor in living cells. J Phys Chem B. 2007; 111:13619–13625. [PubMed: 17997544]

21. Zhang W, Jiang Y, Wang Q, Ma X, Xiao Z, Zuo W, Fang X, Chen YG. Single-molecule imaging reveals transforming growth factor-beta-induced type II receptor dimerization. Proc Natl Acad Sci U S A. 2009; 106:15679–15683. [PubMed: 19720988]

22. Zhang W, Yuan J, Yang Y, Xu L, Wang Q, Zuo W, Fang X, Chen YG. Monomeric type I and type III transforming growth factor-beta receptors and their dimerization revealed by single-molecule imaging. Cell Res. 2010; 20:1216–1223. [PubMed: 20625381]

23. Ulbrich MH, Isacoff EY. Subunit counting in membrane-bound proteins. Nat Methods. 2007; 4:319–321. [PubMed: 17369835]

24. Kang SH, Won K, Chung HW, Jong HS, Song YS, Kim SJ, Bang YJ, Kim NK. Genetic integrity of transforming growth factor beta (TGF-beta) receptors in cervical carcinoma cell lines: loss of growth sensitivity but conserved transcriptional response to TGF-beta. Int J Cancer. 1998; 77:620–625. [PubMed: 9679767]

25. Padua D, Massague J. Roles of TGFbeta in metastasis. Cell Res. 2009; 19:89–102. [PubMed: 19050696]

Highlights

Hesperetin blocks TGFβ ligand-receptor interactions

Hesperetin inhibits downstream TGFβ-signaling

Hesperetin decreases TGFβ-induced cancer cell migration and invasion

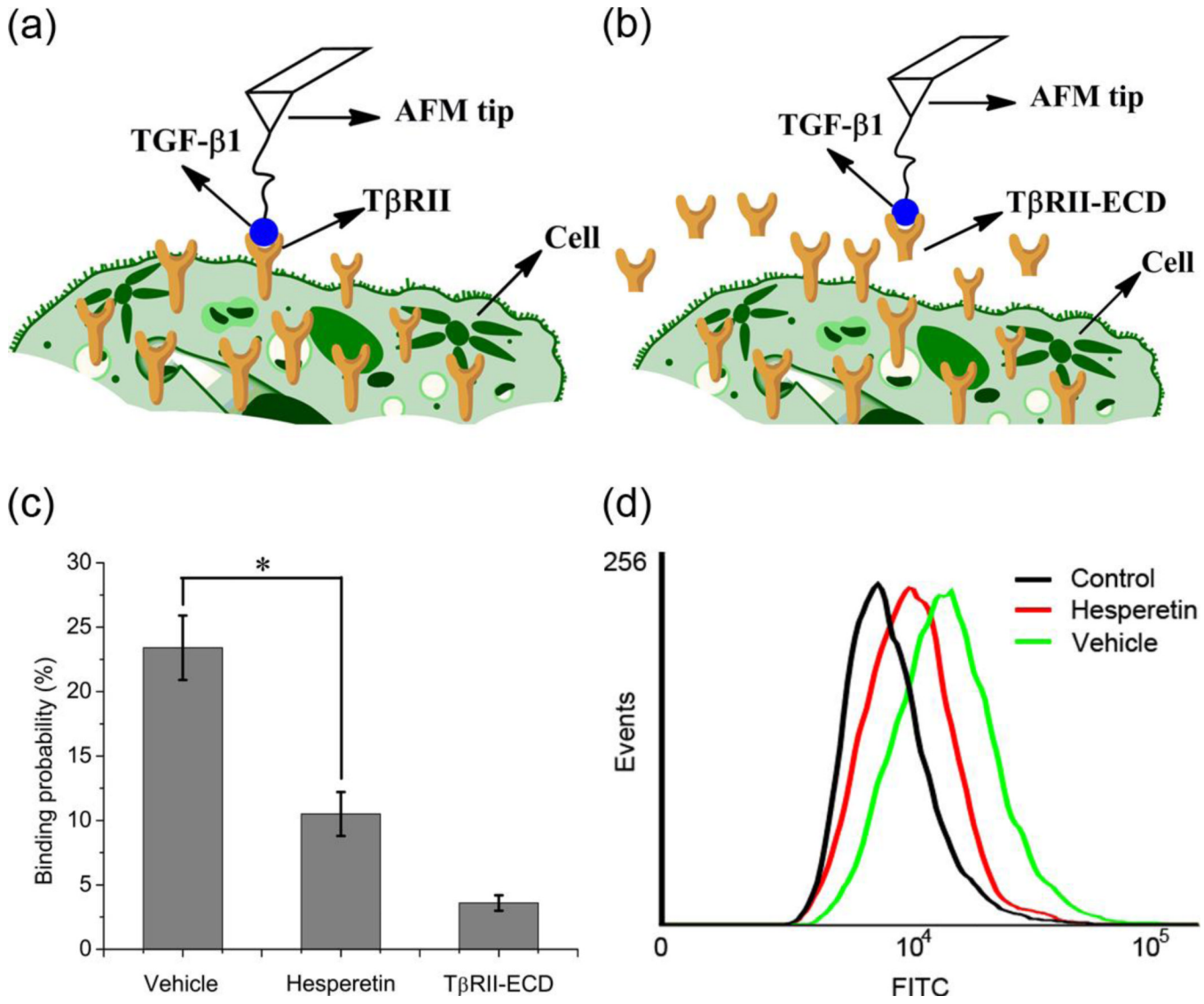

Figure 1.

Measurements of binding between TGF-β1 and TβRII in living cells. (a-b) Schematic diagram of single-molecule force measurements in living cells with a ligand-modified AFM tip in the absence (a) or presence (b) of the extracellular domain of TβRII (TβRII-ECD). The tips were positioned directly above a cell expressing the desired receptors. (c) Binding probabilities derived from AFM force curves. Cells were treated with vehicle (0.1% DMSO), hesperetin (100 nM) or the extracellular domain of TβRII (TβRII-ECD). Data is expressed as mean ±SD. * $P<0.05$. (d) Fluorescence intensity from flow cytometry using biotinylated TGF-β1 and avidin-FITC. Groups comprise vehicle (0.1% DMSO), hesperetin (100 μM) and negative control reagent.

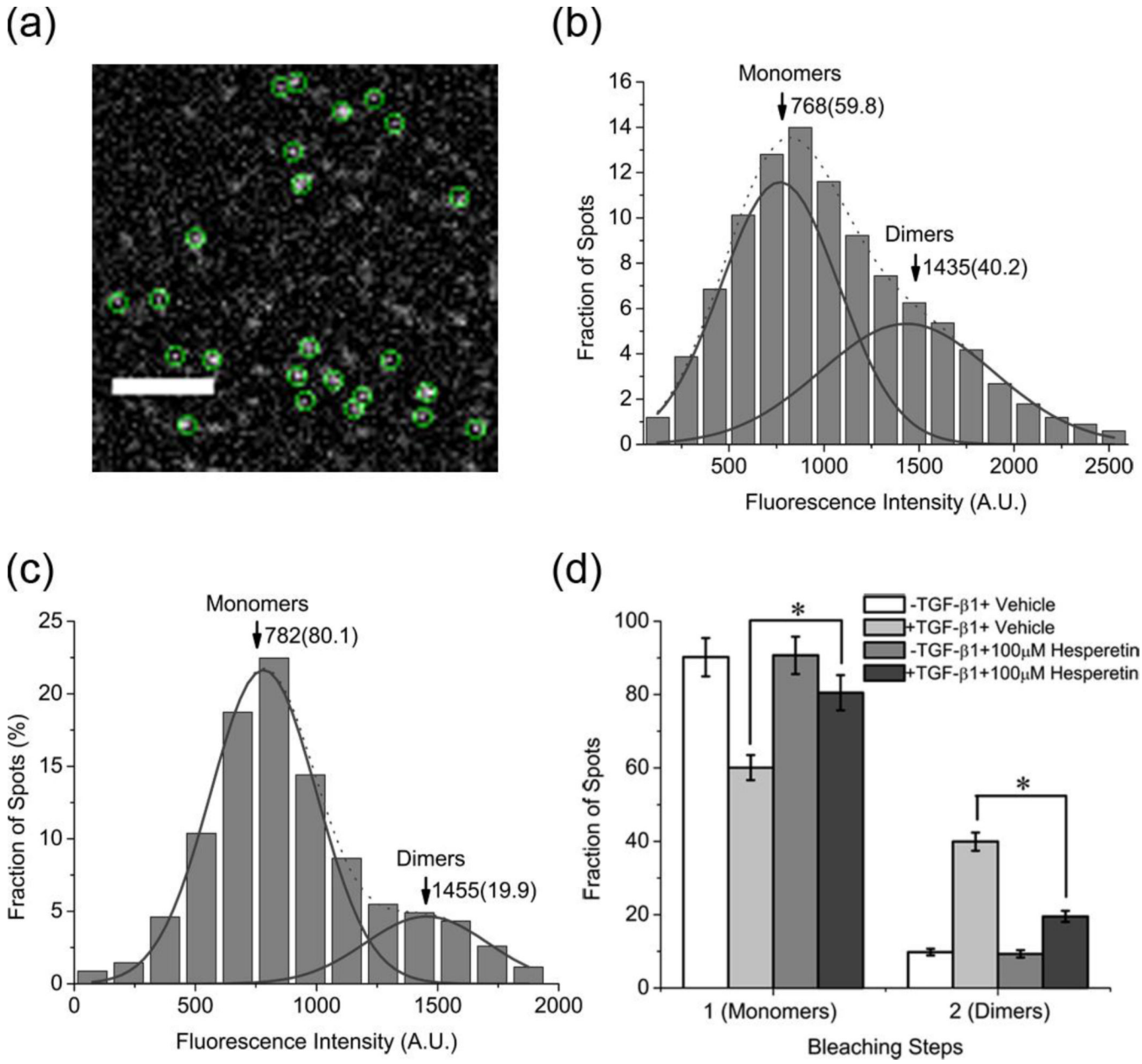

Figure 2.

Measurements of TβRII monomers and dimers. (a) A typical single-molecule fluorescence image of TβRII–GFP molecules on a HeLa cell membrane. Scale bar: 4 μm. (b-c). Fluorescence intensity distribution of individual TβRII–GFP spots on cells incubated with vehicle (0.1% DMSO, N=336) (b) or 100 μM hesperetin (N=347) (c). Solid curves show the fitting of the Gaussian function with the arrowheads indicating peak positions and numbers in parentheses are the respective fractions. (d) Frequency of one- and two-step bleaching events of TβRII-GFP under various conditions. Data is expressed as mean ±SD. * $P<0.05$.

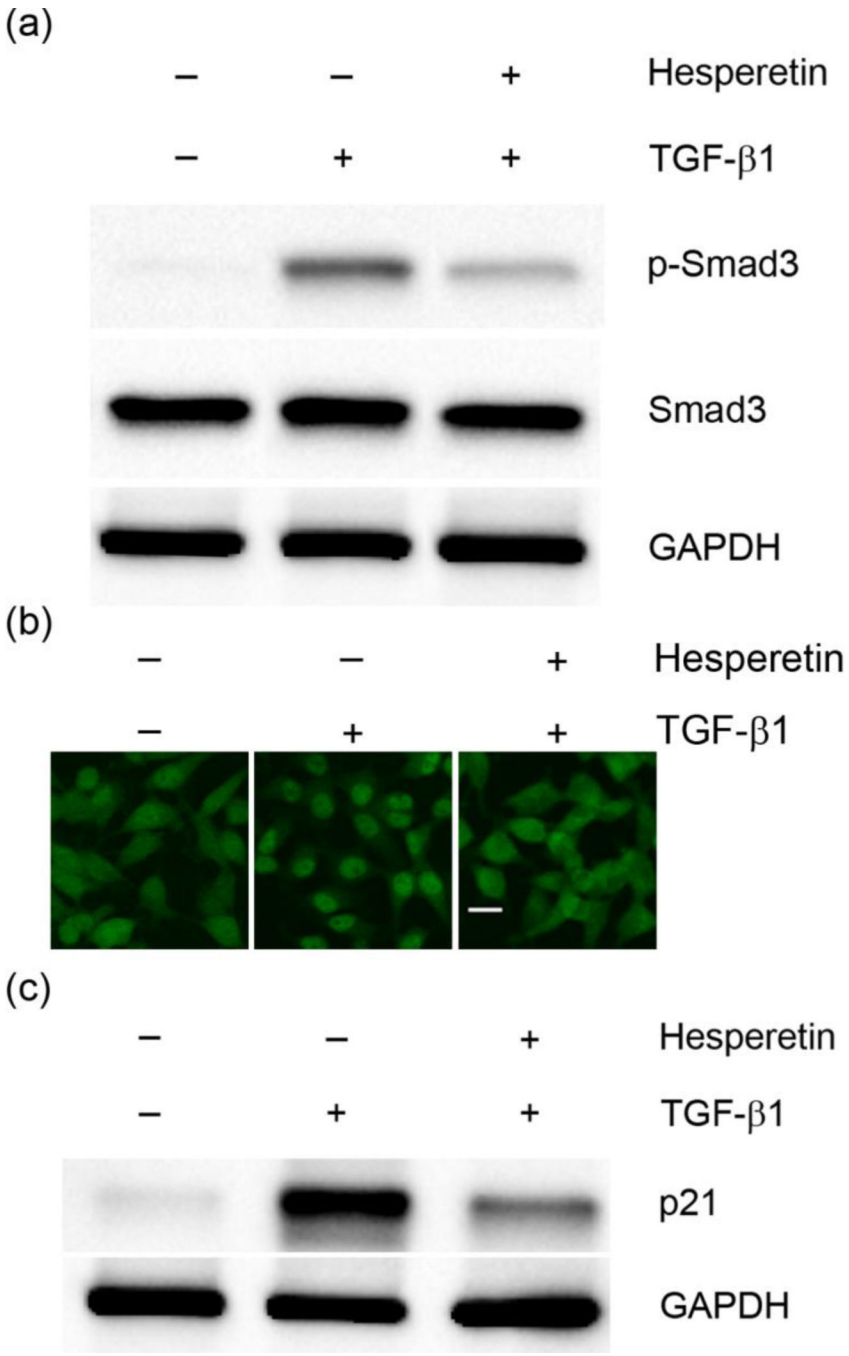

Figure 3.
Effects of hesperetin on TGF-β downstream signaling. (a) Western blot analysis of phosphorylated Smad3 (p-Smad3) in HeLa cell lysates. (b) Immunofluorescence imaging of Smad3. In the presence of hesperetin the nuclear translocation of Smad3 is suppressed. Scale bar: 20μm. (c) Western blot analysis of p21 in HeLa cell lysates.

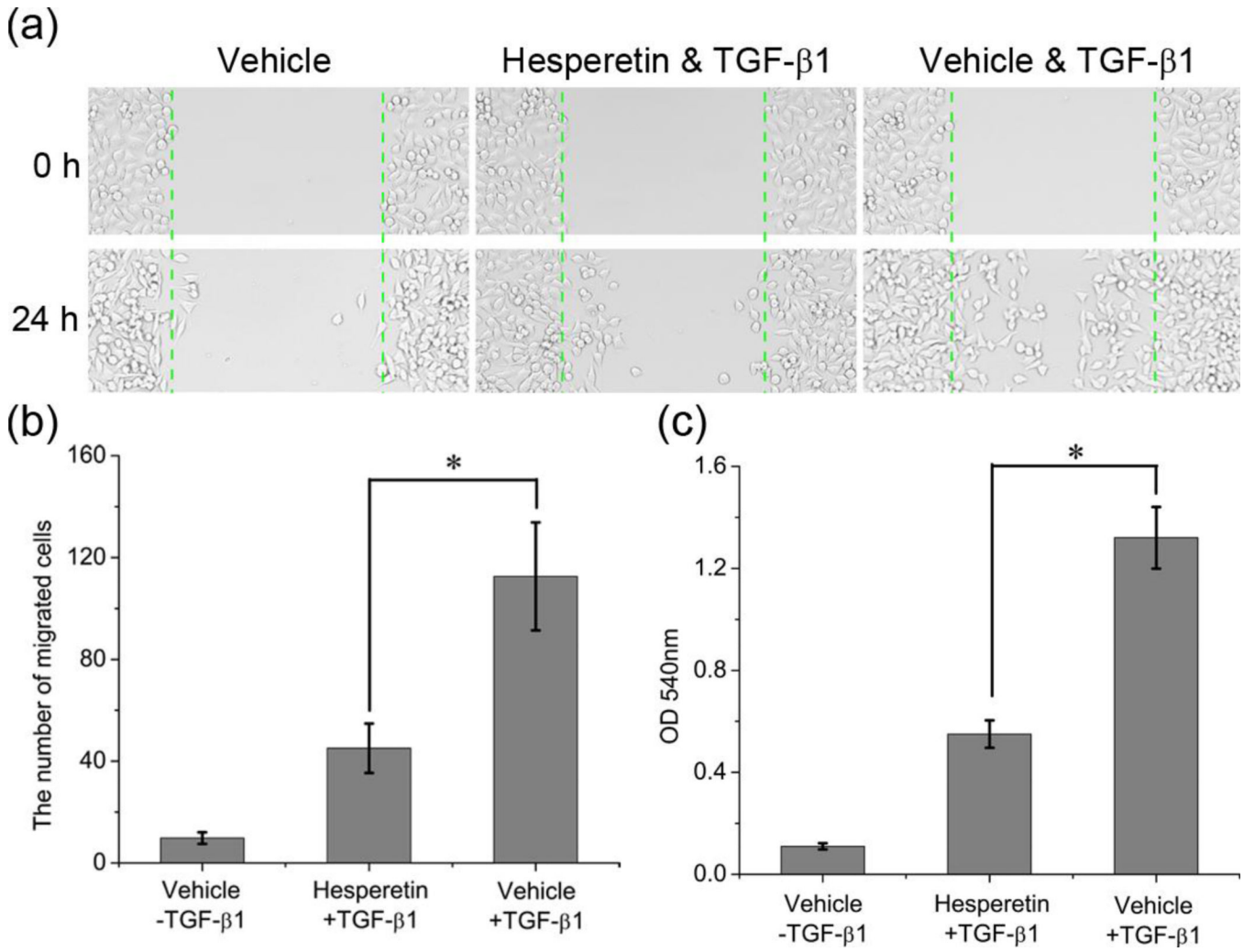

Figure 4.

Evaluation of Hesperetin on TGF-β1-stimulated scattering migration (a-b) and invasion in HeLa cells (Boyden chamber assay) (c). The data represent mean ±SD from three independent analyses. * $P<0.05$.